Supplementary Information

TiO_2-Decorated Titanium Carbide MXene co-Doped with Nitrogen and Sulfur for Oxygen Electroreduction

Haridas Parse,[a,b] Indrajit M. Patil,[a,b] Anita Subhash Swami[b] and Bhalchandra A. Kakade [a,b]*

SRM Research Institute[a], SRM Institute of Science and Technology, Kattankulathur-603 203, Chennai (India)

Department of Chemistry[b], SRM Institute of Science and Technology, Kattankulathur-603 203, Chennai (India)

FAX: (+91) 44-2745 6702

*Corresponding author E-mail: bhalchaa@srmist.edu.in

Figure S1

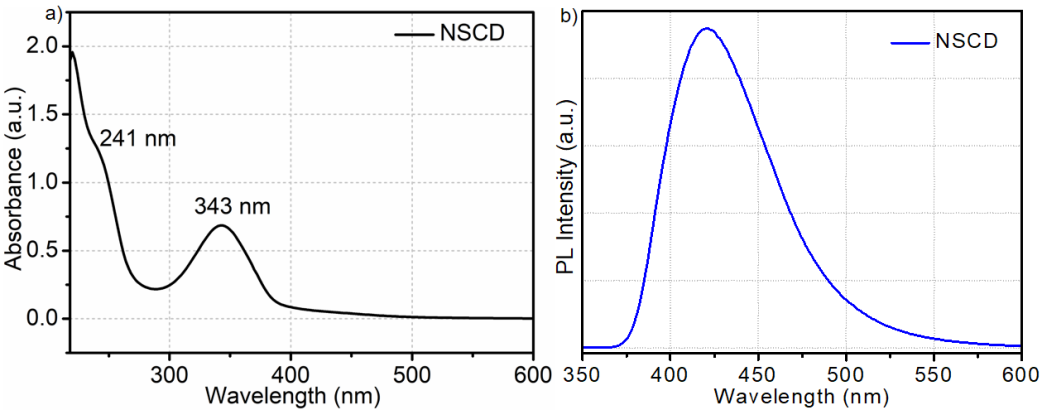

Figure S1.(a) UV-visible spectrum of NSCD; (b) photoluminescence spectrum of as-prepared NSCDs

Figure S2

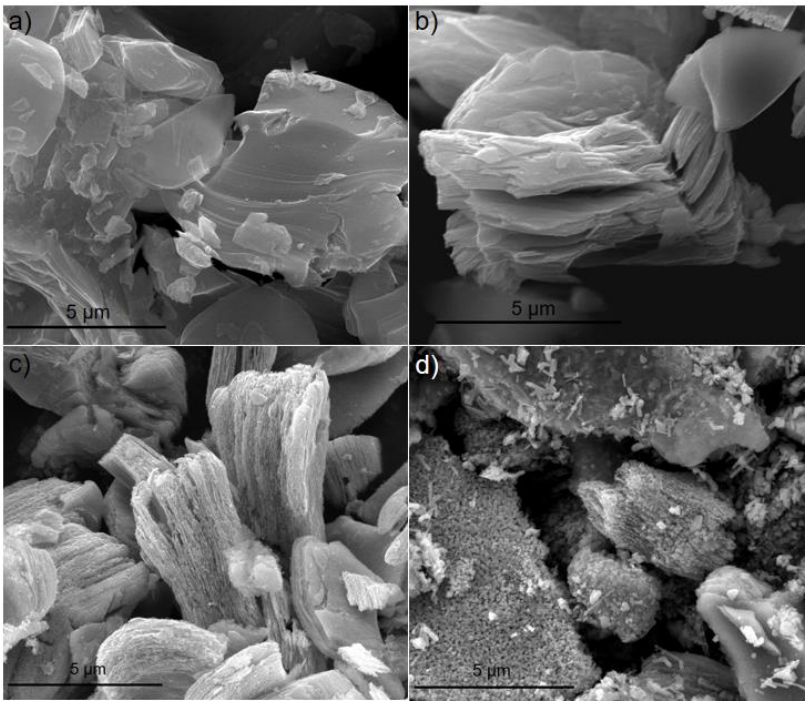

Figure S2. (a-b) SEM images of the pristine Ti_3AlC_2 (MAX phase) and $Ti_3C_2T_x$ (MXene); (c-d) SEM images of the Ti_3C_2/NSCD-500 and Ti_3C_2/NSCD-700.

Figure S3

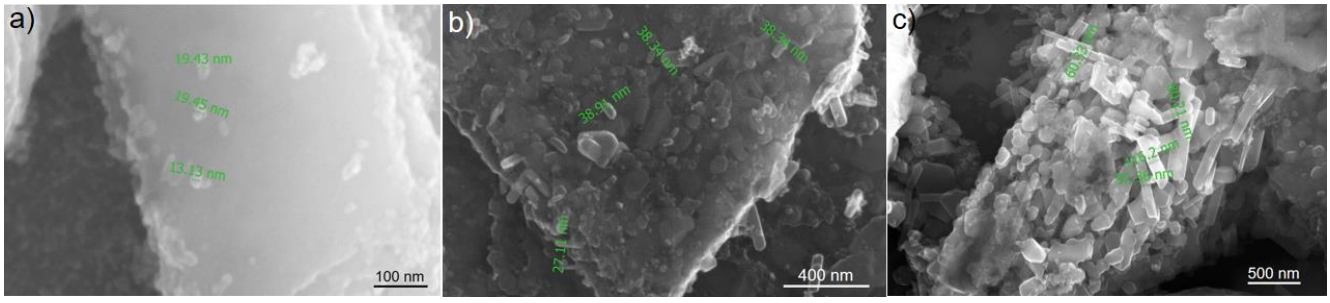

Figure S3. (a-c) SEM images of Ti_3C_2/NSCD-500, Ti_3C_2/NSCD-600, Ti_3C_2/NSCD-700 catalyst (numbers in Fig. indicating the TiO_2 particle size)

Figure S4

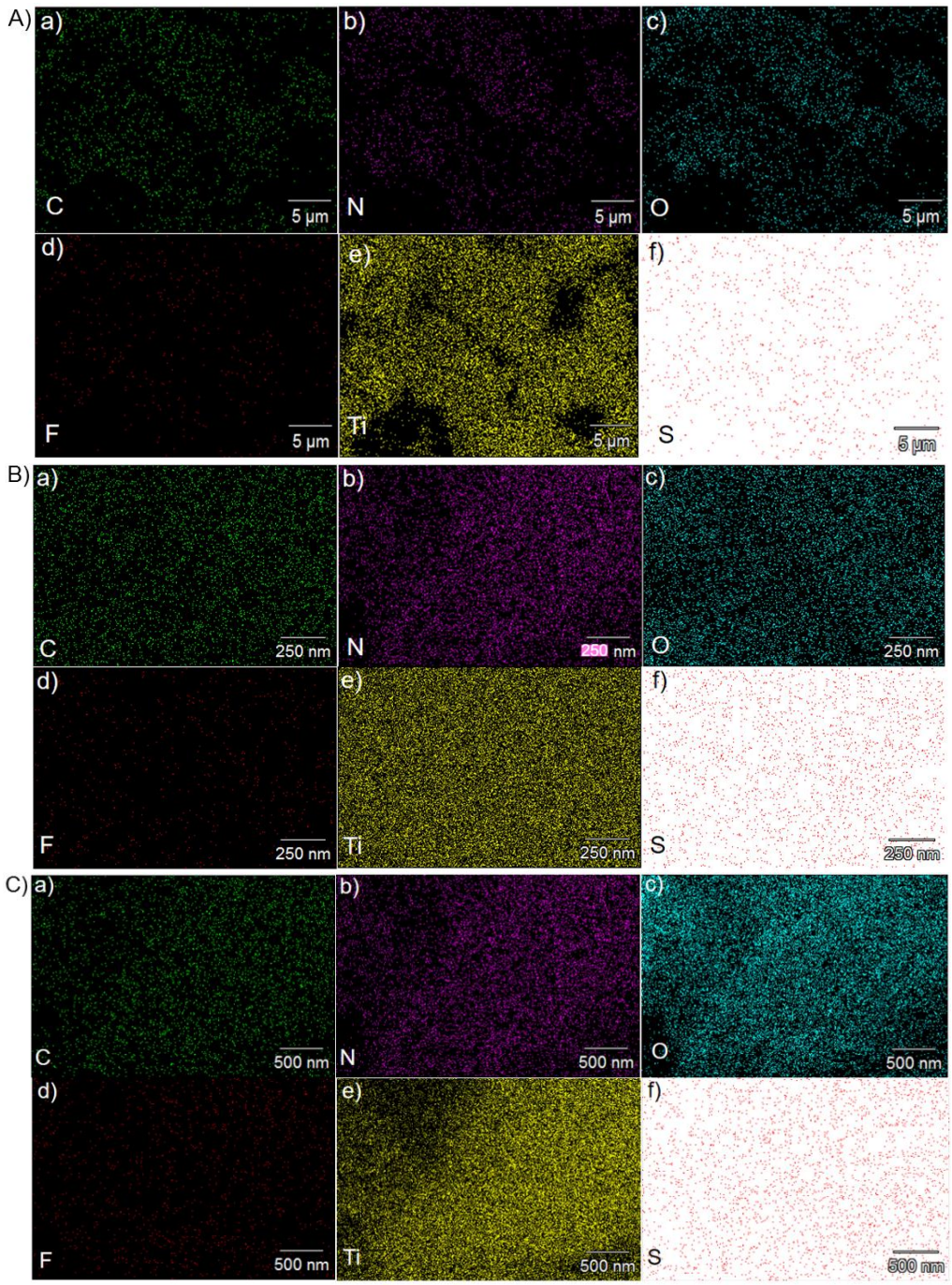

Figure S4. SEM-EDS mapping analysis of A) Ti_3C_2 /NSCD-500, B) Ti_3C_2 /NSCD-600 and C) Ti_3C_2 /NSCD-700 which confirms the uniform distribution of the C, N, O, F, Ti, and S (a-f) elements respectively in A), B), C).

Figure S5

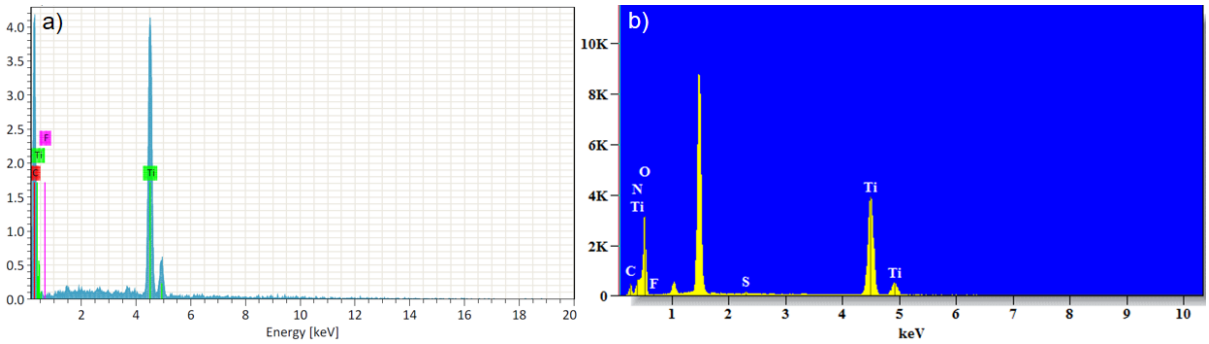

Figure S5. (a)EDS spectrum of the pristine $Ti_3C_2T_x$; (b) EDS profile of nanocomposite Ti_3C_2/NSCD-600.

Figure S6

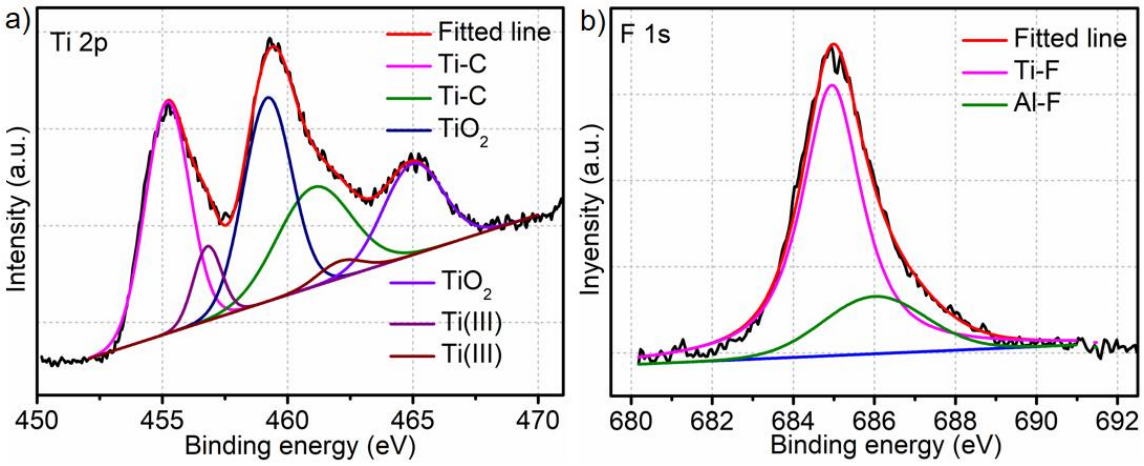

Figure S6. XP spectra of $Ti_3C_2T_x$ deconvoluted core levels for (a) Ti 2p and (b) F 1s.

Figure S7

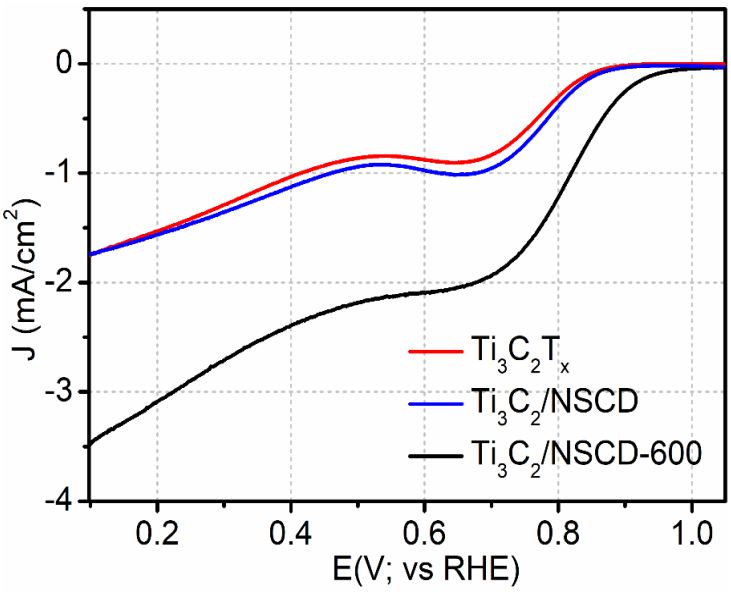

Figure S7. Comparative LSV curves for $Ti_3C_2T_x$, Ti_3C_2/NSCD and Ti_3C_2/NSCD-600 (Step wise electrochemical characterization)

Figure S8

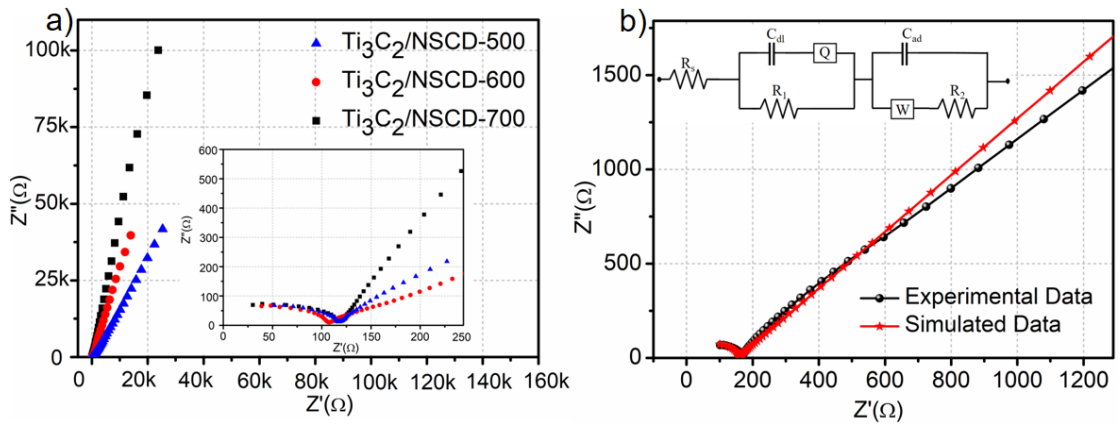

Figure S8. (a) Nyquist plots of the Ti_3C_2/NSCD-500, Ti_3C_2/NSCD-600 and Ti_3C_2/NSCD-700, whereas inset shows high frequency region of EIS; (b) Comparison of experimental and with simulated Nyquist plot of Ti_3C_2/NSCD-600 electrocatalyst.

Figure S9

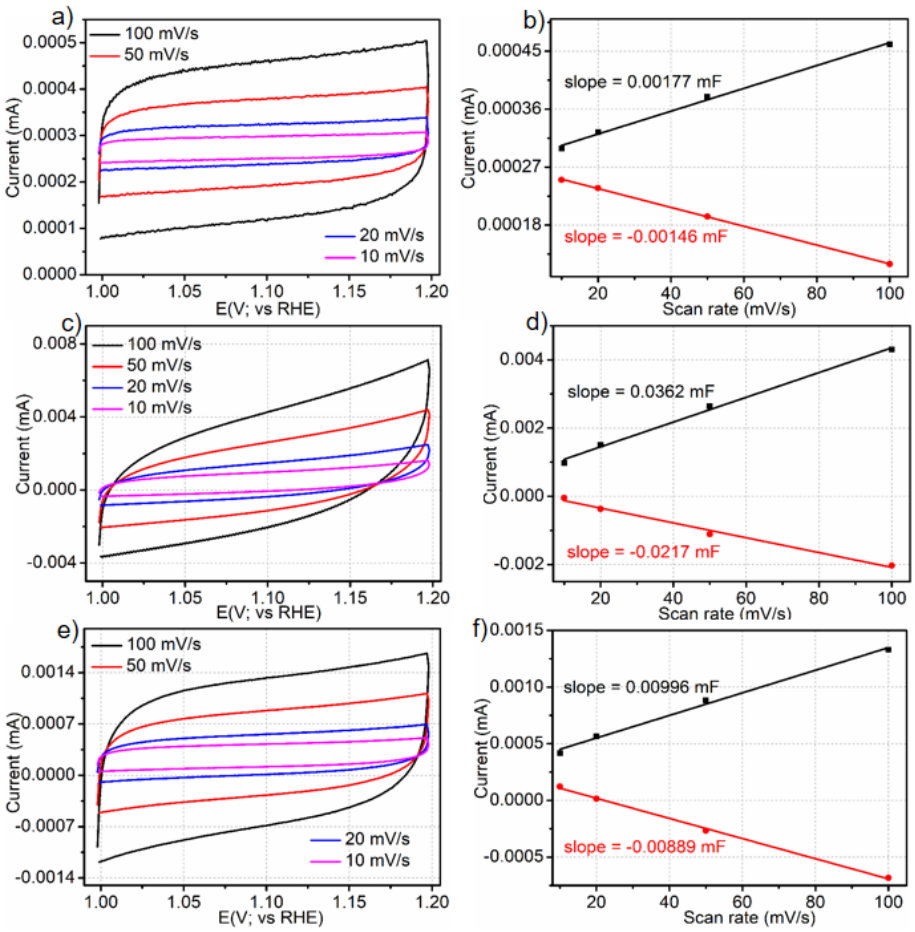

Figure S9. CV curves were recorded in a non-Faradaic region at various scan rates (10 to 100 mV/s) in 0.1 M KOH for (a) Ti_3C_2/NSCD-500 (c) Ti_3C_2/NSCD-600 and (e) Ti_3C_2/NSCD-700. The variations in the current as function of scan rate for (b) Ti_3C_2/NSCD-500 (d) Ti_3C_2/NSCD-600 and (f) Ti_3C_2/NSCD-700 electrode.

Figure S10

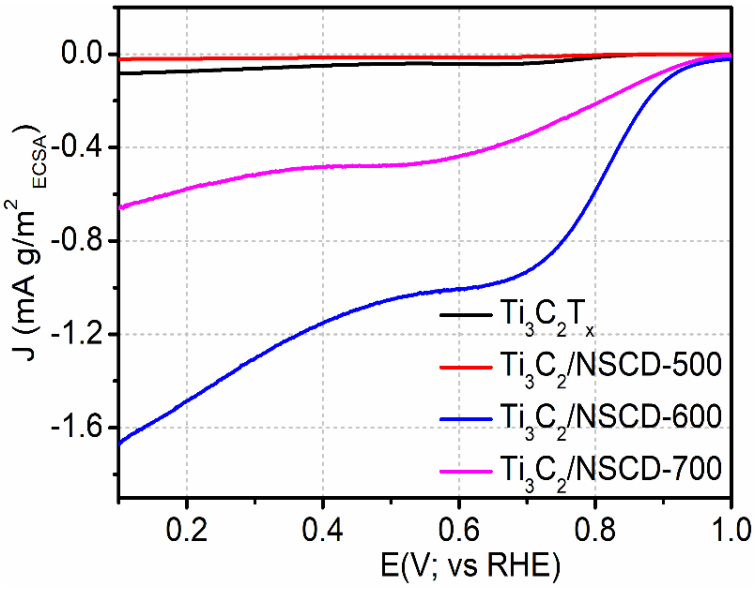

Figure S10. Comparative LSV curves of current density normalized with ECSA value for $Ti_3C_2T_x$ composite prepared at different annealing temperature.

Figure S11

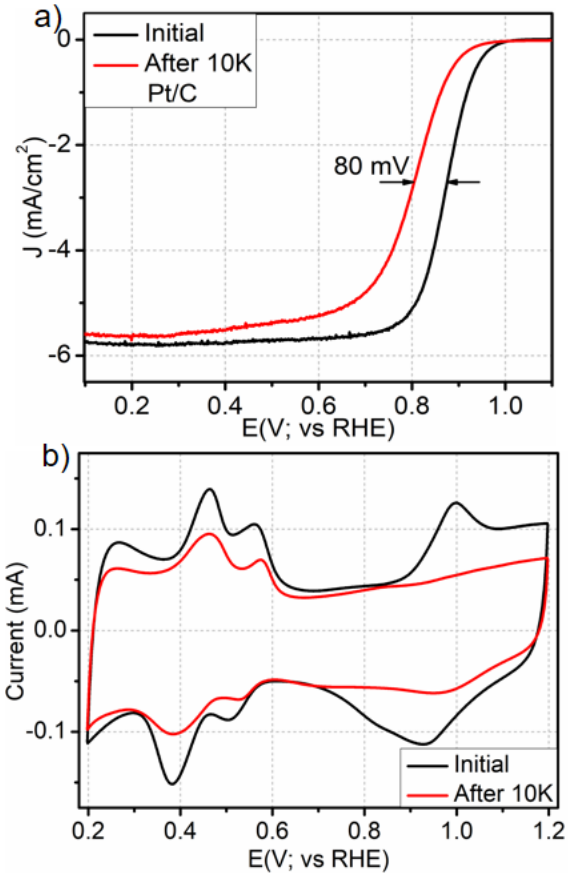

Figure S11. (a) Comparative polarization curves of commercial Pt/C before and after 10k electrochemical cycles at 1600 rpm at 10 mV/s scan rate in alkaline regime (0.1 M KOH); (b) CV curves of the state-of-art catalyst before and after 10k cycles.

Figure S12

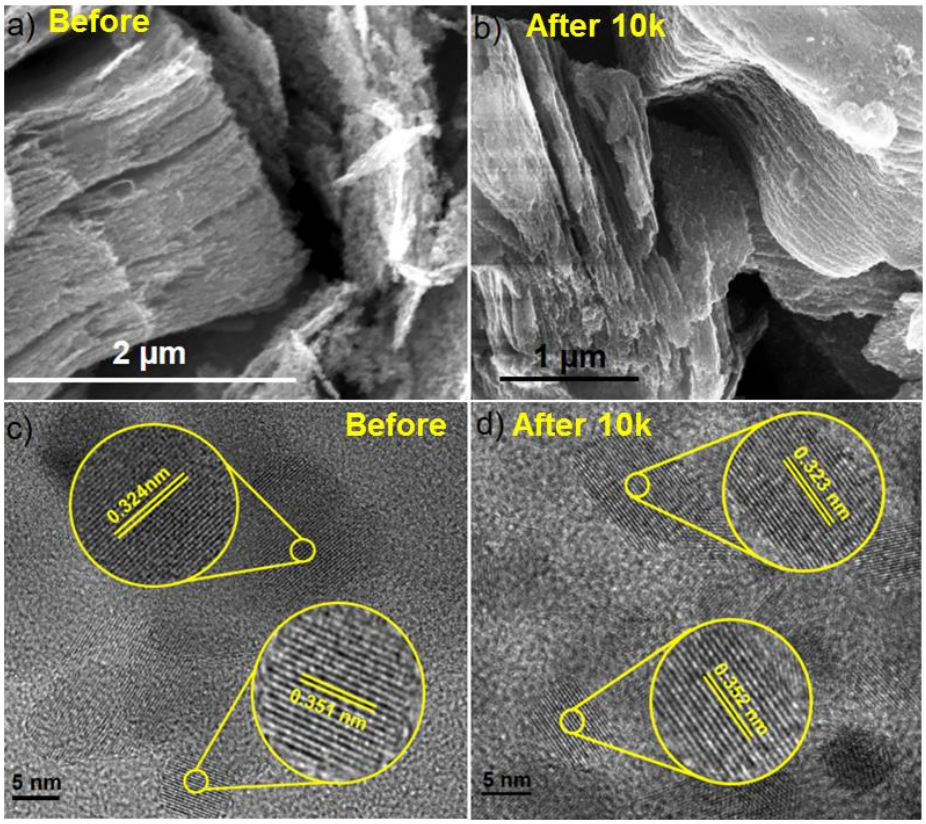

Figure S12. (a-b) SEM and (c-d) HR-TEM images of the Ti_3C_2/NSCD-600 before and after stability test.

Figure S13

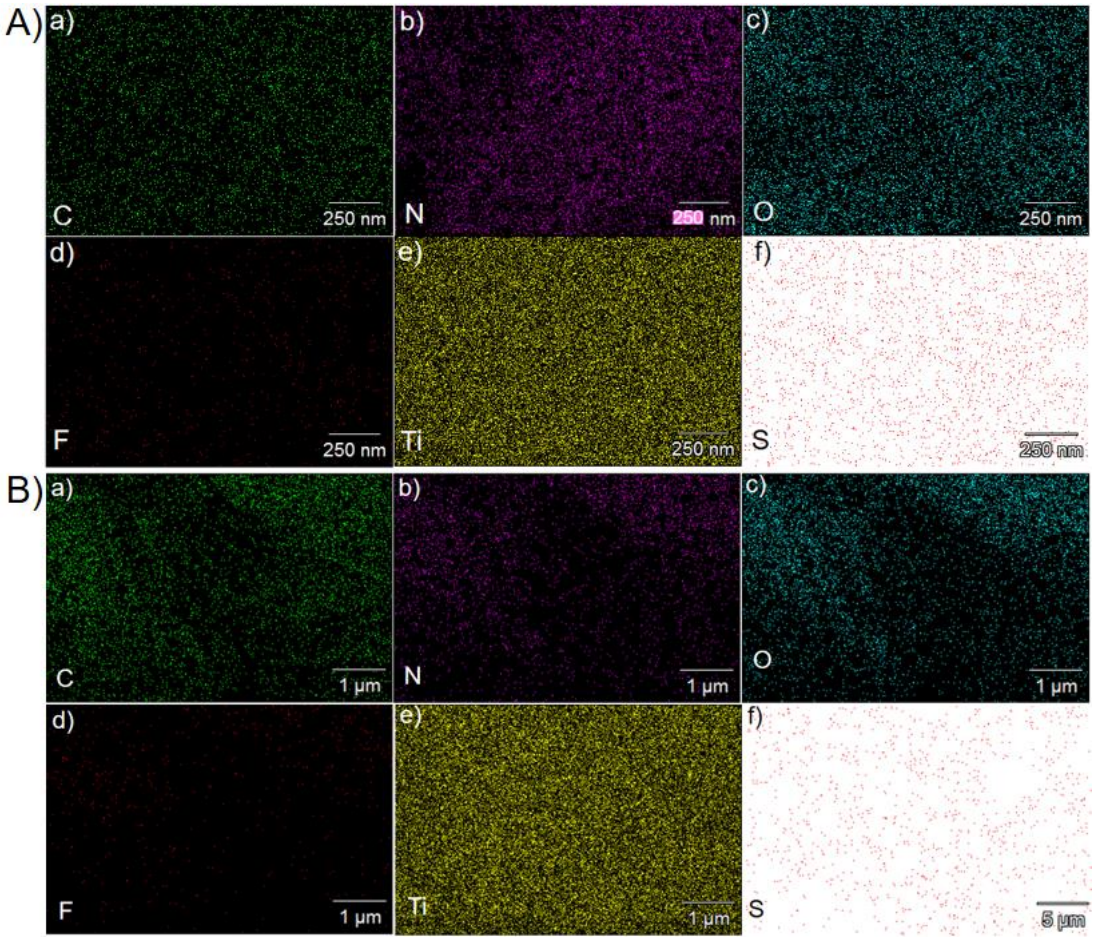

Figure S13. Elemental mapping of Ti_3C_2/NSCD (A) before and (B) after 10k electrochemical cycles which confirms the uniform distribution of the C, N, O, F, Ti, and S (a-f) elements respectively in A) and B) before and after stability .

Table S1

Sr. No.	Catalyst	Electrolyte	Mass loading (mg/cm^{-2})	J_L (mA/cm^2)	$E_{1/2}$ (V) vs RHE	E_{onset} (V) vs RHE	Ref.
1	MXene/NW-Ag0.9Ti0.1	0.1 M KOH	-	4.5	0.782	0.921	[1]
2	$NiCo_2O_4$/MXene	0.1 M KOH	0.700	6.0	0.700	0.920	[2]
3	Mn_3O_4/MXene	0.1 M KOH	0.100	3.5	0.800	0.890	[3]
4	N-doped porous carbons	0.1 M KOH	0.240	5.5	0.840	0.910	[4]
5	Co/N-CNTs@$Ti_3C_2T_x$	0.1 M KOH	0.408	5.8	0.815	0.936	[5]
6	FePc/$Ti_3C_2T_x$	0.1 M KOH	-	5.5	0.850	0.980	[6]
7	Ti-C-T_x	0.1 M KOH	0.120	4.2	0.75	0.870	[7]
8	NSCD/C-600	0.1 M KOH	0.226	5.0	0.71	0.87	[8]
9	N-GQD	0.1 M KOH	-	2.5	0.4	0.75	[9]
10	TiC@NC(0.2)-800	0.1 M KOH	0.120	4.8	0.92	1.08	[10]
11	CNFe	0.1 M KOH	0.600	5.5	0.901	0.998	[11]
12	GQD-MWCNT	0.1 M KOH	-	7.8	0.79	0.81	[12]
13	G-BGQD	0.1 M KOH	-	4.2	0.8	0.94	[13]
14	N-GQDs	0.1 M KOH	-	2.8	0.69	0.79	[14]
15	Co@CoOx/NCNT	0.1 M KOH	0.200	5.5	0.800	0.940	[15]
16	Co-CoO/N-rGO	0.1 M KOH	0.210	5.8	0.880	0.880	[16]
17	Co@NCNT	0.1 M KOH	0.425	6.2	0.828	1.030	[17]
18	NG/CNT/Co_3O_4	0.1 M KOH	-	5.0	-	0.938	[18]
19	**Ti_3C_2/NSCD-600**	0.1 M KOH	**0.240**	**3.5**	**0.8**	**0.98**	**This Work**

Table S1. Electrochemical activity comparison of optimized catalyst and previously reported catalysts.

Table S2

Sr. No.	Sample Code	Sample Name	Mass Activity (mA/mg)
1	A	Ti_3C_2@NSCD-500	91.25
2	**B**	**Ti_3C_2@NSCD-600**	**211.8**
3	C	Ti_3C_2@NSCD-700	180.0
4	D	Ti_3C_2(HT)-600	195.5
5	E	$Ti_3C_2T_x$	77.5
6	F	Pt/C	236.0

Table S2: Comparative mass activity of all composites

References:

1. Zhang, Z.; Li, H.; Zou, G.; Fernandez, C.; Liu, B.; Zhang, Q.; Peng, Q. Self-Reduction Synthesis of New MXene/Ag Composites with Unexpected Electrocatalytic Activity, *ACS Sustain. Chem. Eng.* **2016**, *4*, 6763-6771.
2. Lei, H.; Tan, S.; Ma, L.; Liu, Y.; Liang, Y.; Javed, M. S.; Mai, W. Strongly Coupled $NiCo_2O_4$ Nanocrystal/MXene Hybrid through In Situ Ni/Co–F Bonds for Efficient Wearable Zn–Air Batteries, *ACS Appl. Mater. Interfaces* **2020**.DOI: 10.1021/acsami.0c11185
3. Xue, Q.; Pei, Z.; Huang, Y.; Zhu, M.; Tang, Z.; Li, H.; Zhi, C. Mn_3O_4 nanoparticles on Layer-Structured Ti_3C_2 MXene towards the Oxygen Reduction Reaction and Zinc–Air Batteries, *J. Mater. Chem. A*, **2017**, *5*(39), 20818-20823.
4. Xu, Z.; Zhuang, X.; Yang, C.; Cao, J.; Yao, Z.; Tang, Y.; Feng, X. Nitrogen-Doped Porous Carbon Superstructures Derived from Hierarchical Assembly of Polyimide Nanosheets, *Adv. Mater.* 2016, *28*, 1981-1987.
5. Youkui, Z.; Jiang, H.; Lin, Y.; Liu, H.; He, Q.; Wu, C.; Duan, T.; Song, L. Structural Designs and In-situ X-ray Characterizations of Metal Phosphides for Electrocatalysis, *Adv. Mater. Interfaces* **2018**, 16, 1800392.
6. Li, Z.; Zhuang, Z.; Lv, F.; Zhu, H.; Zhou, L.; Luo, M.; Mai, L. The Marriage of the FeN_4 Moiety and MXene Boosts Oxygen Reduction Catalysis: Fe 3d Electron Delocalization Matters, *Adv. Mater.* 2018, *30*, 1803220.
   DOI: 10.1002/adma.201803220.

7. Parse, H. B.; Moorthi, L.; Patil, I.; Catherin, D.; Marbaniang, P.; Kakade, B. Mixed Phase Titanium Carbide (Ti-C-Tx): A Strategy to Design a Significant Electrocatalyst for Oxygen Electroreduction and Storage Application, *Appl. Surf. Sci.* **2018**, *458*, 819-826. DOI: 10.1016/j.apsusc.2018.07.150
8. Patil, I. M.; Reddy, V.; Lokanathan, M.; Kakade, B. Nitrogen and Sulphur Co-Doped Multiwalled Carbon Nanotubes as an Efficient Electrocatalyst for Improved Oxygen Electroreduction, *Appl. Surf. Sci.* **2018**, *449*, 697-704.
9. Shinde, D. B.; Vishal, V. M.; Kurungot, S.; Pillai, V. K. Electrochemical Preparation of Nitrogen-Doped Graphene Quantum Dots and their Size-Dependent Electrocatalytic Activity for Oxygen Reduction, *Bull. Mater. Sci.* **2015**, *38*, 435-442.
10. Parse, H. B.; Patil, I.; Ingavale, S.; Manohar, C.; Roy, V. A. L.; Kakade, B. Efficient Oxygen Electroreduction Kinetics by Titanium Carbide@ Nitrogen Doped Carbon Nanocomposite, *Int. J. Hydrog. Energy*, **2019,** *44*, 23649-23657.
11. Li, W.; Ding, W.; Jiang, J.; He, Q.; Tao, S.; Wang, W.; Wei, Z. A Phase-Transition-Assisted Method for the Rational Synthesis of Nitrogen-doped Hierarchically Porous Carbon Materials for Oxygen Reduction Reaction J. Mater. Chem. A, 2018, *63*, 878-883. https://doi.org/10.1039/C7TA09435C
12. Zhou, X.; Tian, Z.; Li, J.; Ruan, H.; Ma, Y.; Yang, Z.; Qu, Y. Synergistically Enhanced Activity of Graphene Quantum Dot/Multi-walled Carbon Nanotube Composites as Metal-free Catalysts for Oxygen Reduction Reaction. *Nanoscale* **2014**, *6*, 2603-2607.
13. Van Tam, T.; Kang, S. G.; Babu, K. F.; Oh, E. S.; Lee, S. G.; Choi, W. M. Synthesis of B-Doped Graphene Quantum Dots as a Metal-free Electrocatalyst for the Oxygen Reduction Reaction. *J. Mater. Chem. A*, **2017**, *5*, 10537-10543.
14. Li, Y.; Zhao, Y.; Cheng, H.; Hu, Y.; Shi, G.; Dai, L.; Qu, L. Nitrogen-Doped Graphene Quantum Dots with Oxygen-Rich Functional Groups. *J. Am. Chem. Soc.*, **2012**, *134*, 15-18.
15. Lin, C.; Shinde, S. S.; Jiang, Z.; Song, X.; Sun, Y.; Guo, L.; Lee, J. H. In situ Directional Formation of Co@ Co-Ox-Embedded 1D Carbon Nanotubes as an Efficient Oxygen Electrocatalyst for Ultra-high Rate Zn–Air Batteries. *J. Mater. Chem. A*, **2017**, *5*, 13994-14002. https://doi.org/10.1039/C7TA02215H
16. Liu, X.; Liu, W.; Ko, M.; Park, M.; Kim, M. G.; Oh, P.; Cho, J. Metal (Ni, Co)-Metal Oxides/Graphene Nanocomposites as Multifunctional Electrocatalysts, *Adv. Funct. Mater.* **2015**, *25*, 5799-5808.

17. Zhang, E.; Xie, Y.; Ci, S.; Jia, J.; Cai, P.; Yi, L.; Wen, Z. Multifunctional High-Activity and Robust Electrocatalyst Derived from Metal–Organic Frameworks, *J. of Mater. Chem. A*, **2016**, *4*, 17288-17298.
18. Li, S. S.; Cong, H. P.; Wang, P.; Yu, S. H. Flexible Nitrogen-Doped Graphene/Carbon Nanotube/Co_3O_4 Paper and its Oxygen Reduction Activity, *Nanoscale,* **2014**, *6*, 7534-7541.